The American Journal of Pathology, Vol. 193, No. 2, February 2023

The American Journal of
PATHOLOGY
ajp.amjpathol.org

GASTROINTESTINAL, HEPATOBILIARY, AND PANCREATIC PATHOLOGY

Inhibition of Heat Shock Factor 1 Signaling Decreases Hepatoblastoma Growth via Induction of Apoptosis

Edward H. Hurley,*† Junyan Tao,†‡ Silvia Liu,†‡ Yekaterina Krutsenko,‡ Sucha Singh,‡ and Satdarshan P. Monga†‡

From the Departments of Pediatrics and Pathology,‡ University of Pittsburgh School of Medicine, Pittsburgh; and the Pittsburgh Liver Research Center,† University of Pittsburgh School of Medicine and University of Pittsburgh Medical Center, Pittsburgh, Pennsylvania*

Accepted for publication October 11, 2022.

Address correspondence to Edward H. Hurley, M.D., Division of Newborn Medicine, Department of Pediatrics, University of Pittsburgh School of Medicine, 3240 Craft Pl., Ste. 200, Pittsburgh, PA 15213; or Satdarshan P. Monga, M.D., Department of Pathology, University of Pittsburgh School of Medicine, 200 Lothrop St., S-422 BST, Pittsburgh, PA 15261.
E-mail: ehh9@pitt.edu or smonga@pitt.edu.

Although rare compared with adult liver cancers, hepatoblastoma (HB) is the most common pediatric liver malignancy, and its incidence is increasing. Currently, the treatment includes surgical resection with or without chemotherapy, and in severe cases, liver transplantation in children. The effort to develop more targeted, HB-specific therapies has been stymied by the lack of fundamental knowledge about HB biology. Heat shock factor 1 (HSF1), a transcription factor, is a canonical inducer of heat shock proteins, which act as chaperone proteins to prevent or undo protein misfolding. Recent work has shown a role for HSF1 in cancer beyond the canonical heat shock response. The current study found increased HSF1 signaling in HB versus normal liver. It showed that less differentiated, more embryonic tumors had higher levels of HSF1 than more differentiated, more fetal-appearing tumors. Most strikingly, HSF1 expression levels correlated with mortality. This study used a mouse model of HB to test the effect of inhibiting HSF1 early in tumor development on cancer growth. HSF1 inhibition resulted in fewer and smaller tumors, suggesting HSF1 is needed for aggressive tumor growth. Moreover, HSF1 inhibition also increased apoptosis in tumor foci. These data suggest that HSF1 may be a viable pharmacologic target for HB treatment. *(Am J Pathol 2023, 193: 148–160; https://doi.org/10.1016/j.ajpath.2022.10.006)*

Although rare compared with adult liver cancers, hepatoblastoma (HB) is the most common pediatric liver malignancy, and its incidence is increasing. Currently, the treatment includes surgical resection with or without chemotherapy. However, liver transplantation may be needed in severe pediatric cases; large or invasive tumors require liver transplantation.[1–3] Historically, patients with resectable tumors have a 10-year survival rate of 86% versus only 39% for nonresectable tumors.[4] Between the late 1990s and late 2010s, the percentage of patients receiving liver transplant has increased from 8% to 19%.[2] There is a critical need for hepatoblastoma-specific treatments, but knowledge gaps in the fundamental biology of the tumor have hampered efforts.

A small subset of hepatoblastomas develop in children with genetic conditions such as Beckwith-Wiedemann syndrome or familial adenomatous polyposis.[5,6] However, most cases are believed to be sporadic. For >20 years, it has been known that >80% of hepatoblastomas contain mutations in the *CTNNB1* gene, which encodes β-catenin, an important activator in the Wnt pathway.[7–9] Most mutations that lead to degradation-resistant forms of β-catenin occur in exon 3, a region that contains phosphorylation sites that lead to β-catenin destruction.[10] Our laboratory developed a mouse model of hepatoblastoma based on transfection with constitutively active β-catenin and yes-associated protein 1 (YAP1).[11] YAP1 is an important factor in the Hippo signaling pathway, which is critical in development and controlling organ size.[12,13] Variations of this mouse model show that different β-catenin mutations modulate tumor

Supported by the Pittsburgh Liver Research Center Pilot and Feasibility grant and NIH/National Institute of Diabetes and Digestive and Kidney Diseases P30DK120531 (E.H.H.) and 5R01CA204586-05 (S.P.M.).
Disclosures: None declared.

https://doi.org/10.1016/j.ajpath.2022.10.006

growth and histology.[14,15] Despite decades of research, the exact role of β-catenin signaling in hepatoblastoma is still being elucidated. A review of gene expression data for the β-catenin/YAP1 model showed that signaling for heat shock factor 1 (HSF1) was elevated in tumors.

Over the last decade, there has been a growing appreciation for the role of HSF1 in cancer biology.[16,17] HSF1 expression in breast, colon, and lung cancer correlates with tumor severity.[18–20] HSF1, although traditionally known for its role in counteracting heat-induced misfolding of proteins,[21] is also involved in the expression of genes involved in extracellular matrix formation, DNA repair, cell cycle signaling, apoptosis, and energy metabolism.[17]

HSF1 signaling has been implicated in the development of hepatocellular carcinoma.[22–24] However, little is known about the role of HSF1 in the development and growth of hepatoblastoma. While nuclear HSF1 staining in human hepatoblastoma samples is ubiquitous, it is absent or low in the surrounding normal liver tissue.[25] The canonical role of HSF1 involves stimulation of the heat shock response involving molecular chaperones or heat shock proteins (HSPs) to counteract heat-induced misfolding of proteins.[21] Many other stress signals, including pH changes and radiation, can induce this response.[26,27] Because rapidly proliferating cancer cells experience cytotoxic stress, co-opting the heat shock response can support their survival. However, the role of HSF1 in cancer goes further than mitigating protein folding. Recent work has shown that HSF1 controls another suite of genes related to apoptosis, cell cycle signaling, DNA repair, energy metabolism, and extracellular matrix formation.[17]

A meta-analysis of human hepatoblastoma gene expression sets indicated that HSF1 expression was higher in hepatoblastoma and in more clinically aggressive tumors. HSF1 was inhibited in a mouse model of hepatoblastoma generated by hydrodynamic tail vein injection of mice with plasmids containing constitutively active forms of β-catenin and YAP1 (β-Y model). This led to the development of tumors genetically and histologically reminiscent of hepatoblastoma in the mice.[11,28] HSF1 signaling was inhibited using a dominant negative plasmid (dnHSF1) that forms a truncated protein that can form tumors like native HSF1 but does not activate downstream transcription.[29] This approach has been used to inhibit HSF1 in other cancers, including models of hepatocellular carcinoma.[23,24] The current study demonstrates that inhibiting HSF1 leads to decreased tumor growth in the HB mouse model by induction of increased apoptosis in tumor foci. This work suggests HSF1 may be a viable treatment target and biomarker for hepatoblastoma.

Materials and Methods

Historical RNA-Sequencing Data of β-Catenin/YAP1 Mouse Model

Historical RNA-sequencing set of livers from β-Y model mouse hepatoblastoma model and wild-type controls were analyzed (*https://www.ncbi.nlm.nih.gov/geo/query/acc.cgi?acc=GSE130178*, accession number GSE130178).[15] Tumors used in this study were induced using the model developed by our laboratory based on hydrodynamic tail vein injection of mice with plasmids containing constitutively active forms of YAP1 and β-catenin.[11] Five β-Y and five wild-type control mice were sequenced and analyzed using a NovaSeq 600 instrument (Illumina, Inc., San Diego, CA) by Novagene, Inc. (Sacramento, CA). Identification of differentially expressed transcripts was assessed by three methods: CLC Genomic Workbench version 12.0 (Qiagen, Germantown, MD), DeSeq2 (*http://www.bioconductor.org/packages/release/bioc/html/DESeq2.html*), and edgeR (*https://bioconductor.org/packages/release/bioc/html/edgeR.html*). Only transcripts deemed significant by all methods were included in analysis. To control for multiple comparisons, an adjusted false discovery rate P value was calculated on the basis of the method developed by Benjamini and Hochberg.[30] HSF1 expression levels were compared by performing unpaired t-test using Prism 9.2.0 (GraphPad Software, San Diego, CA). A gene signature associated with activation of HSF1 signaling was applied to the transcriptomic set.[17] Significance was analyzed using the Fisher exact test with Prism. $P < 0.05$ was deemed significant.

Human Hepatoblastoma Samples

To assess the role of HSF1 signaling in human hepatoblastoma, public databases, Gene Expression Omnibus and ArrayExpress, were searched for human transcriptomic data sets measuring RNA expression in hepatoblastoma and controls.[31,32] A total of six sets were identified: GSE131329 (*https://www.sciencerepository.org/gene-expression-profiling-in-hepatoblastoma-cases-of-the-japanese-study-group-for-pediatric-liver-tumors-2-jplt-2-trial_EJMC-2018-1-103*), GSE75271 (*https://aasldpubs.onlinelibrary.wiley.com/doi/10.1002/hep.28888*), E-MEXP-1851 (*https://www.ebi.ac.uk/arrayexpress/experiments/E-MEXP-1851*), GSE81928 (*https://www.nature.com/articles/s42003-018-0077-8*), GSE104766 (*https://aasldpubs.onlinelibrary.wiley.com/doi/10.1002/hep.29672*), and GSE89775 (*https://www.nature.com/articles/srep38347*).[10,33–37] In aggregate, these sets represented a total of 191 livers from patients with hepatoblastoma and 65 normal control livers. This collection included three sets of RNA microarray data and three that used RNA sequencing. Different controls were used in different sets. While some studies used liver samples from patients without hepatoblastoma, others used tissue harvested from nontumor liver areas from patients with hepatoblastoma. The current study used both types of controls. For detailed information about the included gene expression sets, see Supplemental Table S1. For each data set, expression levels of different genes in tumors were compared with control livers using the limma package in R (*https://www.r-project.org*). Finally, meta-analysis was

performed to integrate multiple studies. For each gene, a meta *P* value was calculated by the Fisher method to combine the *P* values in all the six studies for the overall significance evaluation.[38]

Animal Model

Wild-type FVB/N mice were purchased from Jackson Laboratory (Bar Harbor, ME). To induce hepatoblastoma, approximately 6-week−old male mice were injected with plasmids containing constitutively active forms of YAP1 and β-catenin along with the Sleep Beauty transposon/transposase plasmid into the lateral tail vein over 5 to 7 seconds.[11] Each mouse received 20 μg pT3-EF5α-Δ90-β-catenin-Myc-tag and pT3-EF5α-S127A-YAP1-Flag-tag along with the transposase in a ratio of 25:1, diluted in 2 mL of normal saline (0.9% NaCl), filtered through a 0.22-μm filter (MilliporeSigma, Burlington, MA). A dominant negative HSF1 plasmid (dnHSF1) was used to inhibit HSF1 signaling. Mice were also injected with 60 μg of pT3-EF1a-dnHSF1-V5-tag along with the β-catenin and YAP1 plasmids (dnHSF1-β-Y mice). Controls were injected with only β-catenin and YAP1 plasmids (β-Y mice). Normal mice were injected with saline alone. At least three mice per condition were tested. Mice were housed, fed, and monitored in accordance with protocols approved by the Institutional Animal Care and Use Committee at the University of Pittsburgh (Pittsburgh, PA; protocol number 19126451). All animals were carefully monitored for signs of morbidity or discomfort. Close attention was paid to the abdominal girth. Animals were euthanized at specific time points after injection or at the earliest signs of morbidity. Mice were harvested at approximately 10 weeks after injection of plasmids. Body weight and liver weight were measured, and the livers were fixed and embedded in paraffin. A second set of mice were injected with the β-catenin/YAP1/dnHSF1 plasmids and β-catenin/YAP1 plasmids as control and were harvested at 2 weeks after injection to assess early changes in hepatocytes.

Tissue Staining and Immunohistochemistry

Livers were cut into sections (4 μm thick) and stained with hematoxylin and eosin for immunohistochemistry (IHC). Formalin-fixed sections (4 μm thick) were deparaffinized in graded xylene and alcohol and rinsed in phosphate-buffered saline (PBS). To block endogenous peroxidase activity, the sections were incubated in 3% hydrogen peroxide (Sigma, St. Louis, MO). For antigen retrieval, slides were heated in a pressure cooker in citrate buffer followed by blocking with Superblock (ScyTek Laboratories, Logan, UT) for 10 minutes. Sections were incubated overnight at 4°C or 1-hour room temperature with Myc-tag, HSF1, and YAP1 antibodies. Sections were then incubated with species-specific secondary horseradish peroxidase−conjugated antibody (Chemicon, Temecula, CA) for 30 minutes at room temperature. The following antibodies were used for immunohistochemistry: HSF1 (Cell Signaling, Danvers, MA; number 12972; lot number 1), Myc-tag (Cell Signaling; catalog number 3400; lot number 12), V5-tag (eBioscience; Thermo Fisher Scientific, Waltham, MA); catalog number 14679682; lot number 2093237), phosphorylated mammalian target of rapamycin (mTOR) S2448 (Cell Signaling; catalog number 2976; lot number 8), glutamine synthetase (GS; Cell Signaling; catalog number G2781; lot number 096M4864V), and cleaved caspase 3 (Cell Signaling; catalog number 9664; lot number 22).

Measurement of Apoptosis

Tissues from β-Y and d1-β-Y mice harvested 2 weeks after injection were assessed for apoptosis via terminal deoxynucleotidyl transferase-mediated dUTP nick-end labeling (TUNEL) assay and via IHC for cleaved caspase 3. The TUNEL assay was performed using the ApopTag Peroxidase In Situ Apoptosis Detection Kit (MilliporeSigma). Formalin-fixed, paraffin-embedded liver tissue sections were deparaffinized in three changes of xylene, and then rehydrated in decreasing concentrations of ethanol (two washes in absolute ethanol, followed by two washes in 95% alcohol). Subsequently, the slides were immersed in double-distilled water (5 minutes) and PBS. Next, tissues were pretreated with 20 μg/mL solution of Proteinase K (Millipore) for 15 minutes at room temperature; the enzyme was diluted in PBS, and solution was prepared before use. This was followed by two washes in double-distilled water, 2 minutes each. Endogenous peroxidase activity was quenched by treating the slides with 3% H_2O_2 (30% stock from Thermo Fisher Scientific, dissolved in PBS), after which the slides were rinsed twice in two changes of double-distilled water. The slides were treated with equilibration buffer from the kit (1 minute) and incubated with working strength terminal deoxynucleotidyl transferase enzyme (diluted before use in reaction buffer, according to the manufacturer's instructions) in a humidified chamber for 1 hour at 37°C. Next, the slides were incubated for 10 minutes in the kit's stop/wash buffer to quench terminal deoxynucleotidyl transferase activity, followed by incubation with anti-digoxigenin peroxidase-conjugated antibody for 30 minutes at room temperature. Slides were washed twice in PBS and treated with diaminobenzidine peroxidase substrate (Vector Laboratories, Newark, CA) until the color developed. Then, slides were washed in three changes of double-distilled water counterstained with hematoxylin (Fisher Scientific), dehydrated in increasing concentrations of ethanol, followed by incubation in three changes of xylene. Lastly, slides were treated with mounting medium (BioGenex Laboratories, Fremont, CA) and covered with glass coverslips. IHC for cleaved caspase 3 was performed similarly as for other proteins.

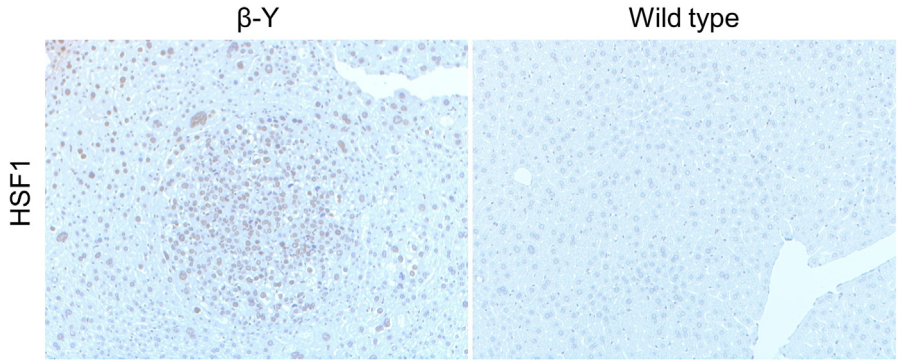

Figure 1 Evaluation of mouse hepatoblastoma model for heat shock factor 1 (HSF1) and activation of downstream genes. Representative images of immunohistochemistry for HSF1 in mouse livers transfected with β-catenin and yes-associated protein 1 (β-Y) plasmids, and wild-type controls showing staining in tumor foci and no staining in wild-type livers. Original magnification, ×10.

In Vitro Transfection of dnHSF1

Approximately 4×10^5 HepG2 cells from ATCC (Manassas, VA) were seeded in 6-well plates (BD Biosciences, Franklin Lakes, NJ). Cells were cultured in Eagle's minimum essential medium (ATCC) supplemented with 10% fetal bovine serum (R&D Systems, Minneapolis, MN). They were transfected with the dnHSF1 or a plasmid containing green fluorescent protein (GFP) as control (1 μg for both) using Lipofectamine 3000 (Thermo Fisher Scientific) using manufacturer's instructions. Transfection efficiency was confirmed by assessing GFP expression in control samples using microscopy. dnHSF1 were compared with control (GFP) livers under basal conditions (37°C) and after heat shock (42°C for 60 minutes, followed by 30 minutes of recovery before harvest).[17] For both sets of experiments, mRNA was extracted from the cells using the RNeasy Mini Kit (Qiagen). mRNA was converted to cDNA and then quantitative PCR was used to assess HSP70 expression using the following forward primer (5′-ACCTTCGACGTGTCCATCCTGA-3′) and reverse primer (5′-TCCTCCACGAAGTGGTTCACCA-3′; Origene, Rockville, MD). Expression of HSP70 was normalized to glyceraldehyde-3-phosphate dehydrogenase and 18S expression using the $\Delta\Delta C_T$ method.[39]

Statistical Analysis

Enrichment of the HSF1 activation code was analyzed using the Fisher exact test. Liver weight/body weight ratio was compared using unpaired *t*-tests using Prism 9 software for Windows (GraphPad Software, Inc.). $P < 0.05$ was considered significant.

Results

HSF1 Target Genes Are Elevated in Mouse Model of Hepatoblastoma

IHC for HSF1 in livers from β-Y model and control mice indicated increased HSF1 staining in tumors compared with normal livers (Figure 1). Historical RNA-sequencing data of the β-Y mouse model showed no increase in HSF1 gene expression in livers from β-Y model mice compared with that in control livers (Table 1). Because HSF1 is a transcription factor and regulates expression of target genes, known transcriptional targets of HSF1 were examined in livers from β-Y model and control mice. *Hspb1* emerged as one of the most differentially expressed genes in the RNA-sequencing data set. *Hspb1* codes for heat shock protein 27 (HSP27), a known transcriptional target of HSF1 (Figure 1). Both HSP27 protein and mRNA are elevated in human hepatoblastoma.[40] There was also a trend toward significant increases for the gene expression of HSP70 (*Hspa4*) and HSP90 (*Hsp90aa1*), the other major heat shock proteins. Finally, transcriptomic data were evaluated for signs of the 456-gene expression signature related to cancer developed by Mendillo et al.[17] Tumors were enriched in this gene set compared with normal livers ($P < 0.0001$, Fisher exact test)

Table 1 Gene Expression Levels of HSF1 and Heat Shock Proteins in a Mouse Model of Hepatoblastoma (GSE130178)

Protein (gene)	Control liver versus mouse HB, fold change	Control liver versus mouse HB, log fold change	Control liver versus mouse HB, *P* value	Control liver versus mouse HB, FDR *P* value
HSF1 (*Hsf1*)	−1.2	−0.2	1.86×10^{-1}	5.71×10^{-1}
HSP27 (*Hspb1*)	−12.0	−3.6	1.34×10^{-14}	1.11×10^{-12}
HSP70 (*Hspa4*)	1.4	0.5	1.20×10^{-2}	6.80×10^{-2}
HSP90 (*Hsp90aa1*)	−1.7	−0.7	2.02×10^{-2}	1.04×10^{-1}

FDR, false discovery rate; HB, hepatoblastoma; HSF1, heat shock factor 1; HSP, heat shock protein.

Table 2 Enrichment of Cancer-Specific HSF1 Signature in a Mouse Model of Hepatoblastoma

Variable	Significant genes	Nonsignificant genes	*P* value
Genes in Mendillo et al[17] signature	143	279	<0.0001
Genes not in Mendillo et al[17] signature	5901	30,010	

Only 422 of the 456 genes in the signature were represented in the entire data set. Only the represented genes (422) were used for statistical analysis.

(Table 2). In summary, expressions of HSF1 target genes were elevated in β-Y mouse model of hepatoblastoma.

HSF1 Signaling Is Increased in Human Hepatoblastoma and Correlates with Less Differentiated and More Lethal Tumors

To directly address clinical relevance, human hepatoblastoma transcriptomic data sets were assessed, as described in *Materials and Methods*. Expression levels of HSF1 were compared between normal tissue and hepatoblastoma tissue using unpaired *t*-test for each of the six sets (Figure 2A). HSF1 expression was significantly increased in tumors over normal livers in three of the six sets. On the basis of the resulting individual *P* values, a meta *P* value was calculated across the sets using the Fisher method adapted from Chang et al.[41] HSF1 expression was significantly elevated in tumors versus normal livers (meta $P = 0.00003$). Next, the study evaluated whether more embryonic, less differentiated tumors had higher levels of HSF1 signaling than fetal-appearing, more differentiated tumors. Studies have shown less differentiated, embryonic-appearing tumors are more clinically aggressive than fetal-appearing, more differentiated tumors.[42,43] Cairo et al[10] showed that a 16-gene panel can distinguish more differentiated, fetal-appearing tumors (C1) from less differentiated, embryonic-appearing tumors (C2). This 16-gene panel was applied across all six gene sets. Levels of HSF1 signaling in C1 and C2 samples were compared using unpaired *t*-tests. HSF1 expression was significantly elevated in C2 tumors compared with C1 tumors in four of the six individual sets. The meta *P* value calculated across all sets indicated that HSF1 was significantly elevated in C2 samples (meta $P = 0.0027$) (Figure 2B).

Finally, the study investigated whether HSF1 expression levels correlated with mortality. Three of the transcriptomic data sets included mortality data (E-MEXP-1851, GSE131329, and GSE75271).[10,33,34] Tumor samples were startified in those sets into quartiles for HSF1 expression. Mortality in the highest quartile was compared with the lowest three quartiles using a Fisher exact test and one of the three was significantly elevated ($P < 0.05$). Calculation of the meta *P* value across all three sets indicated a significant relationship (meta $P = 0.00269$) (Figure 3). HSF1 expression levels were higher in hepatoblastoma than in normal liver. Less differentiated, embryonic-appearing tumors have higher HSF1 levels than more differentiated, fetal-like tumors. High levels of HSF1 expression in tumors correlated with higher mortality rate.

Gene Expression Levels of Individual Heat Shock Proteins Are Elevated in Human Hepatoblastoma

HSF1 modulates a wide suite of genes controlling a variety of cellular functions. Whether HSF1's role in hepatoblastoma may depend on stimulating specific heat shock proteins, its classic pathway, was evaluated. Specifically, tumors versus control livers were compared for gene expression levels of HSP27 (*Hspb1*), HSP70 (*Hspa4*), and HSP90 (*Hsp90aa1*). All three genes were enriched in tumors versus normal livers ($P < 0.05$, unpaired *t*-test) (Supplemental Table S2). Notably, HSP27 was highly significant. Next, correlation between levels of HSPs and differentiation of the tumors was evaluated. HSP27 signaling did not correlate with tumor differentiation for any gene set. HSP70 significantly correlated with differentiation in three of the six sets. Four of the six HSP90 sets correlated with tumor differentiation. Meta *P* values for both HSP70 and HSP90 were significant (Supplemental Table S3). Finally, expression levels of specific HSPs correlated with mortality. Tumors were ordered by level of gene expression and the highest quartile was compared with the lowest three quartiles (Supplemental Table S4). Only one HSP, HSP90, was mildly elevated (meta $P = 0.015$). Overall, although multiple HSPs are elevated in tumors versus normal liver, only a couple distinguish C1 from C2 tumors and only one is minimally correlated with mortality.

HSF1 Performs Better than Myc and Similar to AFP as a Biomarker for Hepatoblastoma

Much work has demonstrated the role of Myc signaling in hepatoblastoma.[40,44] Myc is a transcription factor that is implicated in most cancers and is a transcriptional target of the Wnt/β-catenin pathway. Hepatoblastoma tumors show increased Myc staining.[45] In a mouse model of hepatoblastoma, knocking out Myc decreased tumor growth, suggesting Myc signaling plays a role in β-catenin–mediated tumor growth.[46] Myc signaling correlation with tumors, histology, and mortality was studied next. Lower Myc expression levels were found in tumors versus normal livers (meta $P = 2.24 \times 10^{-6}$) (Supplemental Table S2). Myc levels were not significantly different between embryonic- and fetal-appearing tumors (Supplemental Table

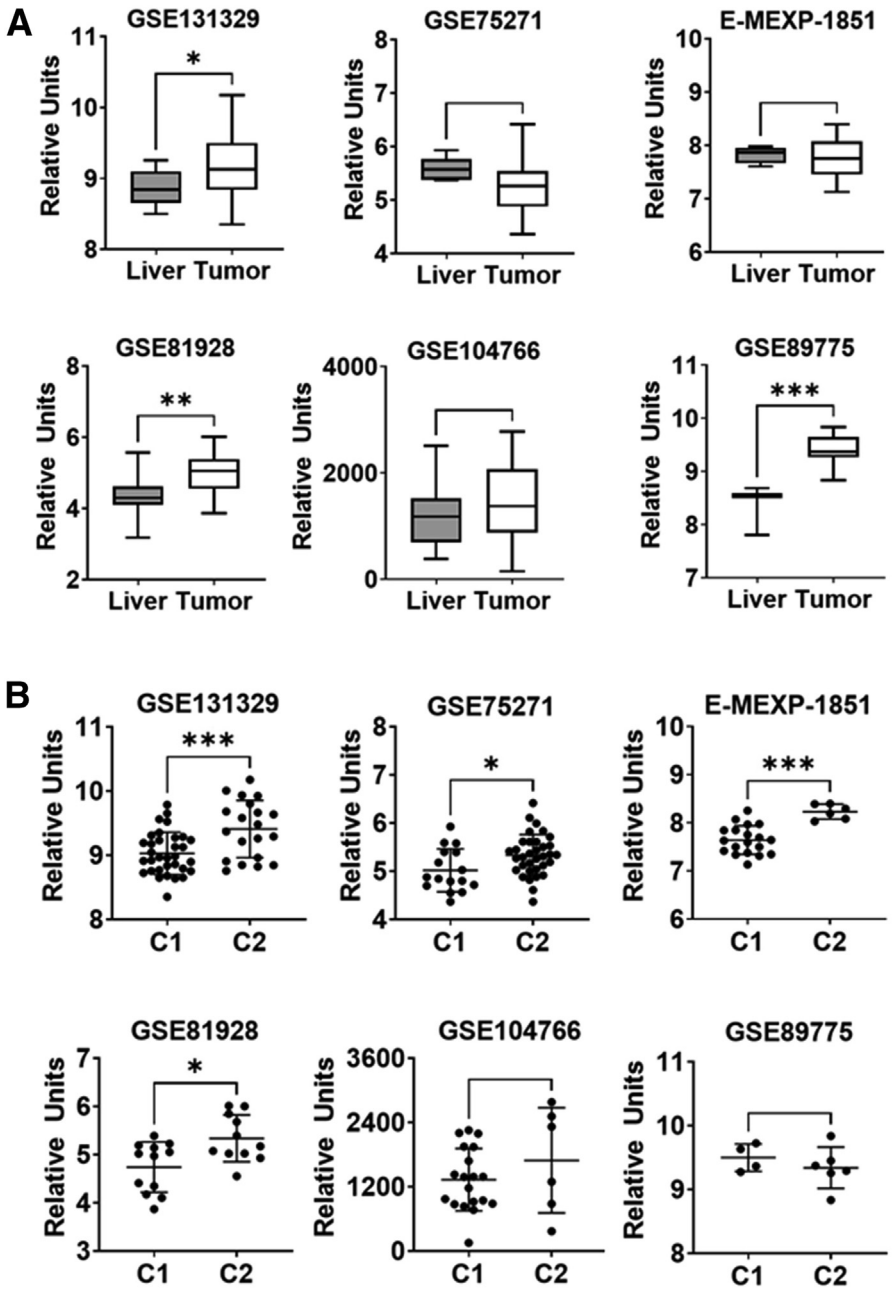

Figure 2 Expression of heat shock factor 1 (HSF1) in overall tumors and in more fetal- or embryonic-appearing tumors. **A:** Expression levels of HSF1 in tumors versus control livers in six transcriptomic data sets: GSE131329 (*https://www.sciencerepository.org/gene-expression-profiling-in-hepatoblastoma-cases-of-the-japanese-study-group-for-pediatric-liver-tumors-2-jplt-2-trial_EJMC-2018-1-103*), GSE75271 (*https://aasldpubs.onlinelibrary.wiley.com/doi/10.1002/hep.28888*), E-MEXP-1851 (*https://www.ebi.ac.uk/arrayexpress/experiments/E-MEXP-1851*), GSE81928 (*https://www.nature.com/articles/s42003-018-0077-8*), GSE104766 (*https://aasldpubs.onlinelibrary.wiley.com/doi/10.1002/hep.29672*), and GSE89775 (*https://www.nature.com/articles/srep38347*). Levels were compared using unpaired *t*-test for each of the six sets. A meta *P* value was then calculated across all sets based on Chang et al[41] (meta $P = 3 \times 10^{-5}$). **B:** Expression levels of HSF1 in tumors differentiated by degree of differentiation, as based on Cairo et al.[10] C1 tumors are more fetal appearing, whereas C2 tumors are more embryonic appearing. Expression levels were compared using unpaired *t*-test. Meta *P* value was calculated across all sets (meta $P = 2 \times 10^{-8}$). $^{*}P < 0.05$, $^{**}P < 0.01$, and $^{***}P < 0.001$.

S3). Myc expression levels in tumors did not correlate with mortality (Supplemental Table S4). Thus, Myc gene expression appears lower in tumors and does not correlate with tumor differentiation or mortality. Next, expression of α-fetoprotein (AFP) across the six gene sets was examined. AFP is a well-known biomarker for HB that is used clinically for screening, monitoring treatment response, and assessing prognosis. AFP expression was elevated in hepatoblastoma versus normal liver (meta $P = 4.05 \times 10^{-25}$) (Table 2). More embryonic tumors (C2) had higher levels of

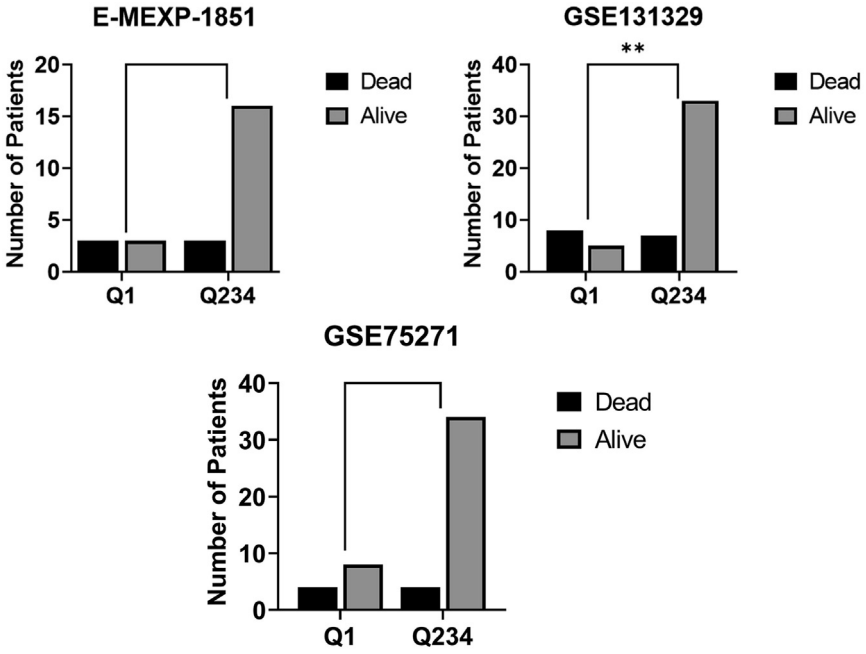

Figure 3 Correlation between heat shock factor 1 (HSF1) expression levels and mortality. Three of the examined transcriptomic data sets featured mortality data: GSE131329 (*https://www.sciencerepository.org/gene-expression-profiling-in-hepatoblastoma-cases-of-the-japanese-study-group-for-pediatric-liver-tumors-2-jplt-2-trial_EJMC-2018-1-103*), GSE75271 (*https://aasldpubs.onlinelibrary.wiley.com/doi/10.1002/hep.28888*), and E-MEXP-1851 (*https://www.ebi.ac.uk/arrayexpress/experiments/E-MEXP-1851*). Expression levels of HSF1 in tumors were ordered and divided into quartiles (Qs). The mortality rate in the quartile with the highest HSF1 expression was compared with the lowest three quartiles using the Fisher exact test for each data set. Mortality was significantly elevated in the highest quartile in one set (GSE131329). A meta *P* value was then calculated across all sets (meta $P = 0.0027$). $^{**}P < 0.01$.

AFP than C1 tumors (meta $P = 8.98 \times 10^{-16}$) (Supplemental Table S3). Tumor expression of Myc was also ordered into quartiles. Similar to HSF1, the quartile of tumors with the highest AFP gene expression had a higher mortality rate than the lowest three quarters (meta $P = 0.0018$) (Supplemental Table S4). In summary, AFP gene expression is higher in tumors versus normal and in embryonic tumors versus fetal-appearing tumors, with high expression levels in tumors associated with increased mortality.

HSF1 Inhibition Prevents HB Development in β-Catenin—YAP1 Mouse Model

A dominant negative for HSF1 was injected along with constitutively active β-catenin and YAP1 plasmids (dnHSF1-β-Y mice) to suppress HSF1 signaling. Mice injected with just β-catenin and YAP1 plasmids served as control (β-Y mice). The latter developed abdominal distention requiring euthanasia by 10 weeks after injection. Mice injected with the dnHSF1 appeared normal as late as 16 weeks after injection. Grossly, livers from the β-Y mice were much larger, paler, and nodular than livers from the dnHSF1-β-Y mice (Figure 4A). Interestingly, dnHSF1-β-Y mice were similar in appearance to wild-type mice injected with only saline. The body weight for β-Y, dnHSF1-β-Y, and wild-type mice did not differ significantly by one-way analysis of variance (Figure 4B). However, when liver/body weight ratio, a measurement of tumor burden, was calculated, higher ratios in β-Y mice versus the dnHSF1-β-Y mice ($P < 0.05$) were found. In fact, liver/body weight ratios for the dnHSF1-β-Y and wild-type mice were similar.

Hematoxylin and eosin—stained liver sections were examined and IHC was performed for Myc-tag, a marker for the β-catenin plasmids, for sections from both β-Y and dnHSF1-β-Y mice (Figure 4C). Sections from β-Y mice showed large tumors, with tightly packed nuclei. These resembled crowed fetal hepatoblastoma, a more embryonic form of the tumor. Hematoxylin and eosin evaluations of dnHSF1-β-Y mice livers showed rare, small tumor foci. The cells appeared more differentiated. These foci showed positive staining for Myc-tag, suggesting they were induced by the β-Y plasmids rather than naturally occurring spontaneous tumors. Early tumors in our mouse model showed positive IHC staining for GS and phosphorylated mTOR, but by 10 weeks after injection, the staining is absent (Supplemental Figure S1).[11] Moreover, using plasmids encoding different β-catenin mutations resulted in more differentiated tumors that showed persistent positive staining for GS and phosphorylated mTOR. To further define the differences between the tumors from β-Y mice and dnHSF1-β-Y mice, GS and phosphorylated mTOR staining was performed. The small foci in dnHSF1-β-Y mice were positive for both, whereas mature β-Y mice tumors showed negative staining for both proteins.

Finally, IHC was performed for plasmid markers to ensure that the current findings did not result from nondelivery of plasmids or off-target effects of the dnHSF1. For both sets of mice, tumor foci showed positive IHC staining for Myc-tag, a synthetic sequence on our β-catenin plasmid. Staining for V5-tag, a label on our dnHSF1 plasmid, was performed next. At 2 weeks after injection, Myc-tag and V5-tag staining was observed in the same foci (Figure 5). Finally, whether the presence of the dnHSF1 persisted in livers well past injection, an indication of whether the

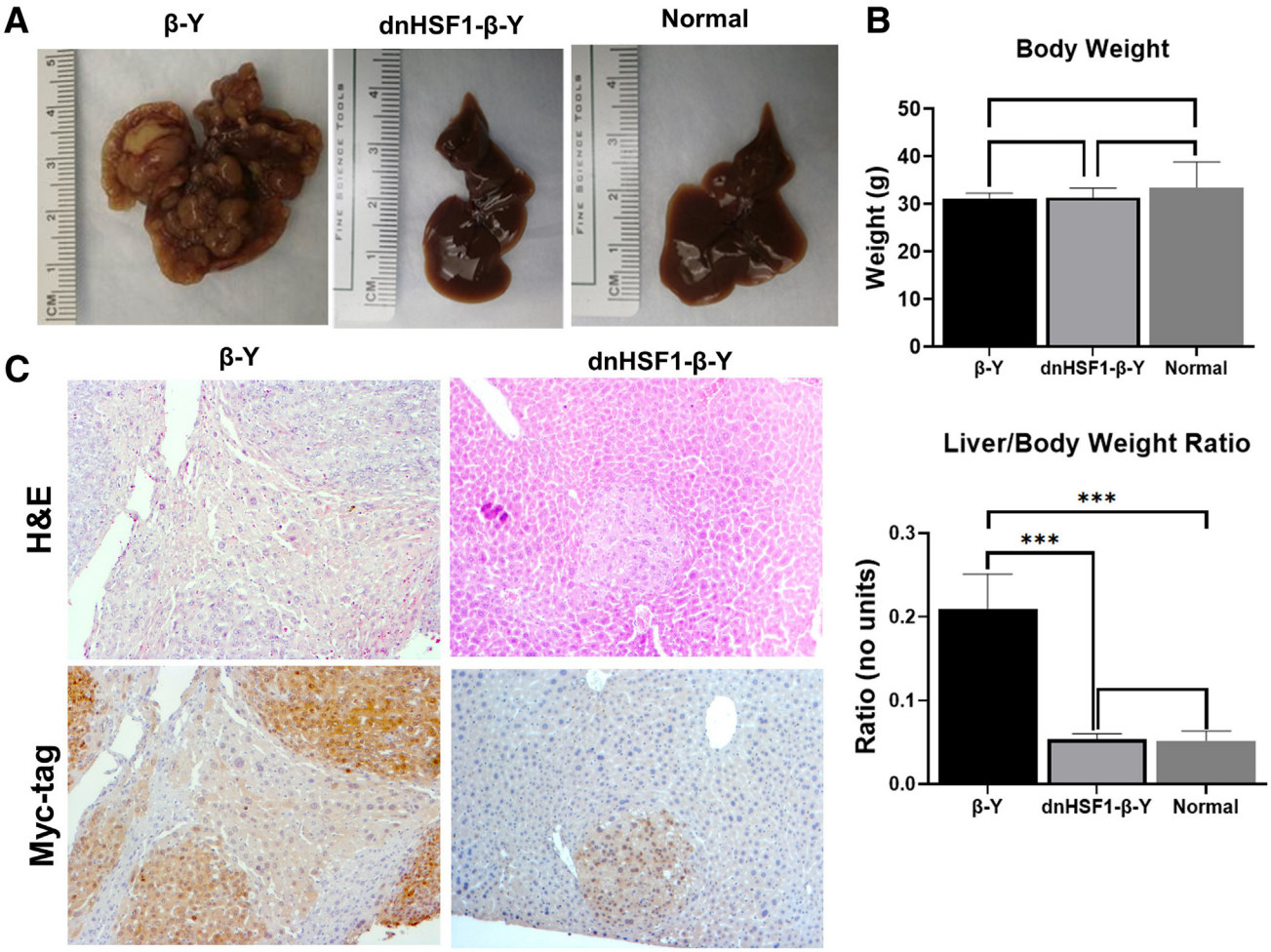

Figure 4 Analysis of livers in mice transfected with a dominant negative for heat shock factor 1 (HSF1) along with constitutively active β-catenin and yes-associated protein 1 (YAP1) plasmids (dnHSF1-β-Y mice) and mice transfect with just β-catenin and YAP1 (β-Y mice) as control. **A:** Representative gross images of mice transfected with β-catenin and YAP1 plasmids (**left panel**), dominant negative HSF1 (dnHSF1), β-catenin and YAP1 plasmid (**middle panel**), and wild-type control (**right panel**). **B: Top panel:** Average body weights of dnHSF1-β, β-Y, and wild-type mice analyzed by one-way analysis of variance. **Bottom panel:** Liver/body weight ratio was calculated and then compared by one-way analysis of variance. **C:** Representative images for hematoxylin and eosin (H&E) staining for β-Y mice and dnHSF1-β-Y mice (**right panels**) and immunohistochemistry for Myc-tag, an artificial tag on the β-catenin plasmid (**left panels**). ***$P < 0.001$. Original magnification, ×10 (**C**).

presence of the dnHSF1 was noxious to the cells, was assessed. IHC of tumors 10 weeks after injection showed persistent staining for V5-tag (dnHSF1; data not shown). In summary, co-injection of the dnHSF1 along with constitutively active β-catenin and YAP1 plasmids decreased tumor burden and led to more differentiated tumor foci.

Inhibition of HSF1 Increases Apoptosis in Early Tumor Foci

To quantify TUNEL and cleaved caspase 3 staining, the number of positive cells was counted in at least 20 high-powered fields for three replicates per condition (β-Y versus the dnHSF1-β-Y). The average number of positive cells per field was calculated and compared using unpaired *t*-test. The dnHSF1-β-Y samples had about three times more staining for both TUNEL and cleaved caspase 3 than the β-Y samples (unpaired *t*-test, $P < 0.05$) (Figure 6). Increased cleaved caspase 3 and TUNEL staining was observed in livers from dnHSF1-β-Y mice versus β-Y mice (unpaired *t*-test, $P < 0.05$). Overall, transfection with the dnHSF1 resulted in increased TUNEL and cleaved caspase 3 staining.

Dominant Negative HSF1 Decreases HSF1 Transcriptional Targets under Stressful Conditions

To address the role of HSF1 in HB biology, HepG2 cells were transfected with the dnHSF1 or GFP as control. As indicated by quantitative PCR, expression of HSP70 was similar between control cells transfected with GFP and dnHSF1 transfected cells under basal conditions. Under heat shock, HSP70 transcription was dramatically increased

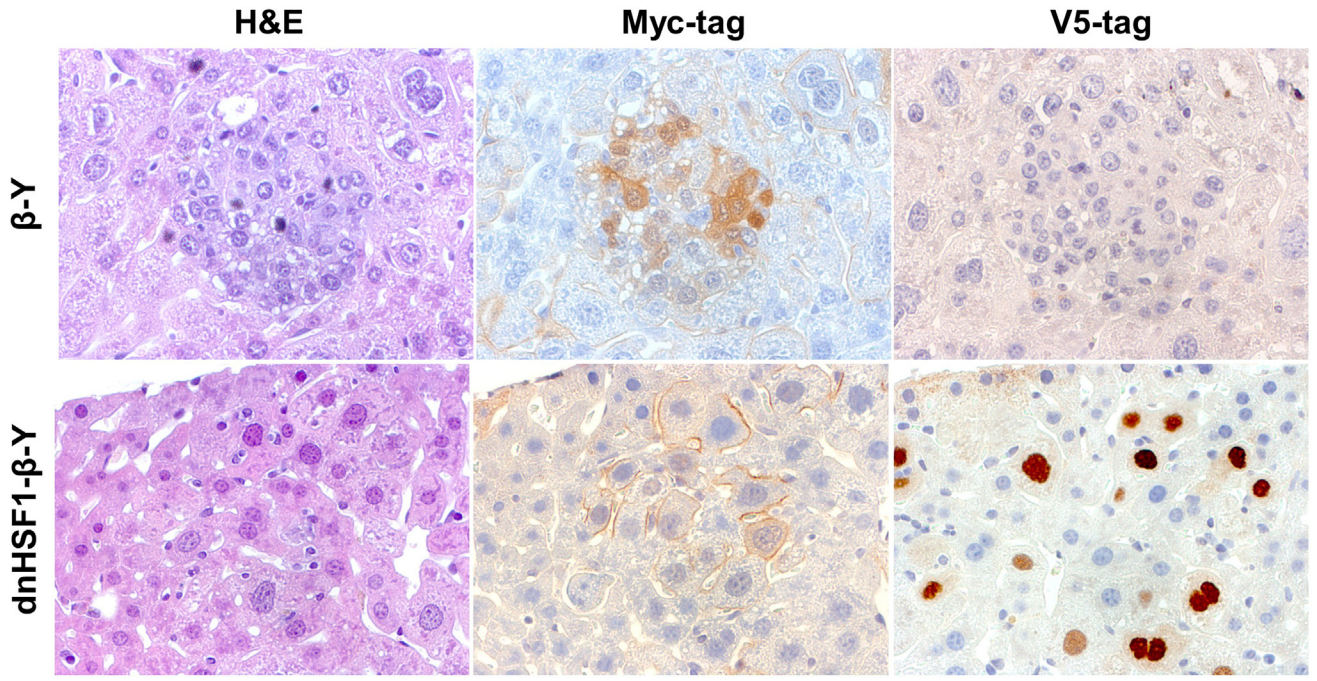

Figure 5 Verification of transfection at 2 weeks after injection. Livers from both constitutively active β-catenin and yes-associated protein 1 (YAP1) plasmids (dnHSF1-β-Y) and β-catenin and YAP1 (β-Y) mice were harvested 2 weeks after injection with the plasmids. Livers from both sets of mice were stained with hematoxylin and eosin (H&E; **left panels**), and immunohistochemistry was performed for Myc-tag (**middle panels**) and V5-tag (**right panels**). V5-tag is an artificial tag on the dnHSF1 plasmid. Original magnification, ×20.

compared with basal conditions for both dnHSF1 and GFP cells (Supplemental Figure S2). However, the increase in HSP70 expression was significantly less in samples transfected with the dnHSF1 compared with control cells ($P < 0.05$, unpaired *t*-test). In summary, transfection of HepG2 cells with the dnHSF1 decreased the expression of HSP70 under stressful conditions.

Discussion

This study demonstrates HSF1 activation in human hepatoblastoma and correlates with tumor differentiation and mortality. Performing a meta-analysis of existing hepatoblastoma gene expression sets provided the statistical power to explore such questions. This work adds to the growing list of cancers associated with HSF1 signaling.[18–20] This study suggests that HSF1 is potentially as good a biomarker as AFP and appears better than Myc. It is unclear why Myc signaling was lower in the tumors in this study versus normal control livers. To fully validate the clinical utility of HSF1 as a biomarker, more work is needed correlating HSF1 protein levels and post-translational modifications with patient data. This analysis suggests HSF1's role in hepatoblastoma is not strictly mediated via induction of HSPs. Genes for HSPs, such as HSP27, HSP70, and HSP90, were increased in hepatoblastoma compared with normal livers. In the case of HSP27, gene expression was highly significant (meta $P = 1.78 \times 10^{-23}$). However, only HSP90 expression correlated with tumor differentiation and mortality, two clinically relevant parameters. These findings suggest HSF1 signaling in hepatoblastoma may encompass both canonical and cancer-specific gene targets. Additional studies interrogating individual HSPs and non-HSP HSF1 target genes are needed to tease which proteins are critical to hepatoblastoma development and growth.

This study also suggests HSF1 may be a viable pharmacologic target for hepatoblastoma. Inhibition of HSF1 in our mouse model of hepatoblastoma significantly decreased tumor formation. The residual tumor foci were significantly fewer and smaller. Histologically, they appeared more differentiated (or less dedifferentiated). Interestingly, the tumor foci in the dnHSF1 mice remained GS-positive after 10 weeks postinjection, whereas control β-Y mice animals were only GS-positive early in tumor development. Generally, more differentiated, fetal-appearing tumors express GS, whereas less differentiated embryonal tumors stain GS-negative.[14] Previously, this approach significantly decreased tumor formation in mouse models of hepatocellular carcinoma based on overexpression of AKT and Myc.[23,24] Interestingly, transfection of the dnHSF1 in a mouse model of hepatoblastoma based on constitutively active β-catenin and transcriptional coactivator with PDZ-binding motif (TAZ) rather than YAP1 did not prevent tumor formation.[25] This discordance is potentially related to the intrinsic differences in YAP1 and TAZ signaling.[47]

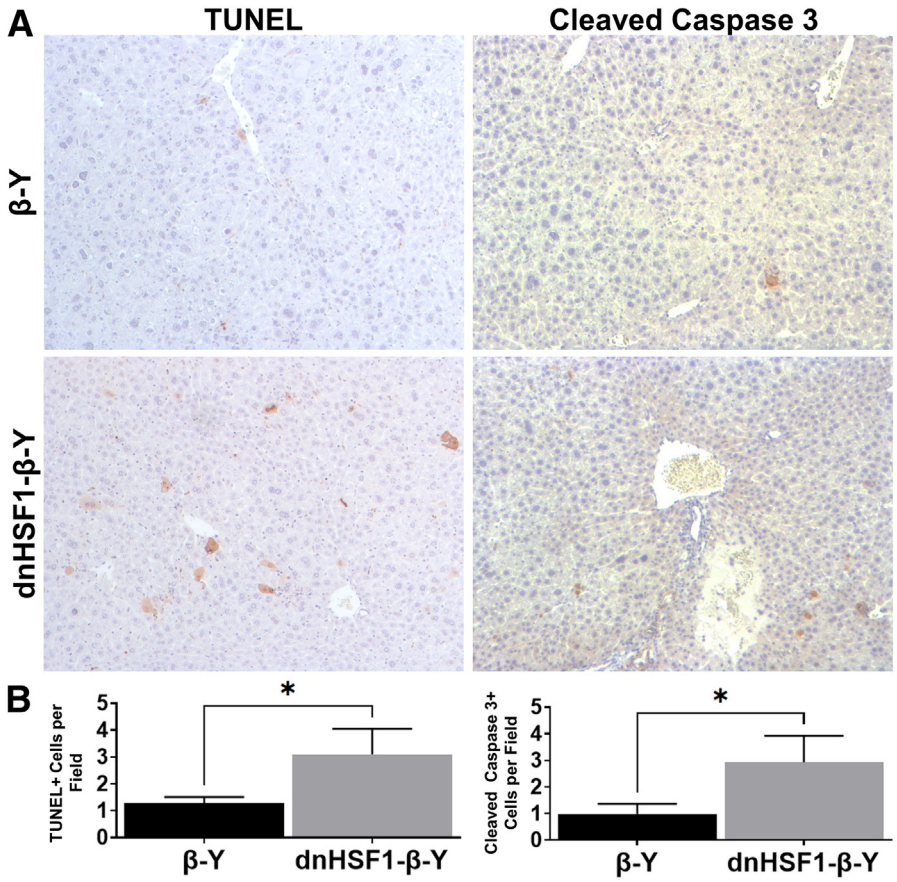

Figure 6 **A:** Terminal deoxynucleotidyl transferase-mediated dUTP nick-end labeling (TUNEL) assay and immunohistochemistry for cleaved caspase 3 were performed on β-catenin and yes-associated protein 1 (YAP1; β-Y) and constitutively active β-catenin and YAP1 plasmid (dnHSF-β-Y) livers from mice harvested 2 weeks after transfection. **B:** TUNEL and cleaved caspase 3 staining was quantified by counting the number of positively stained cells in at least 20 high-powered fields per condition. The average number of positive cells in β-Y and dnHSF-β-Y livers was compared using unpaired *t*-test. $^{*}P < 0.05$. Original magnification, ×10 (**A**).

A drawback of this current study is that HSF1 signaling was inhibited at the time of transfection with β-catenin and YAP1. More studies are needed, including inhibition of HSF1 signaling after tumors have formed. Currently, there are no US Food and Drug Administration–approved HSF1 or HSP inhibitors to treat cancer. Over the last 20 years, inhibitors of various HSF1 downstream targets have been studied as cancer treatments. HSP90 inhibitors, in particular, have been extensively studied as cancer treatment in human trials, but limited treatment response and adverse effects limited their utility.[48] HSP70 inhibitors have also been tested with similar disappointing results.[49,50] Antisense oligonucleotides to HSP27 have been developed and tested in patients with urothelial and lung cancer.[51,52] Experimentally, known small-molecule HSF1 inhibitors, such as N^2-(1H-indazole-5-yl)-N^6-methyl-3-nitropyridine-2,6-diamine (KRIBB11) and direct targeted HSF1 inhibitor (DTHIB), have been shown in mouse models and cell culture to decrease cancer growth, but they have not been tested in humans.[53,54] In early 2022, a phase 1 clinical trial for NXP800, an oral HSF1 inhibitor, began recruitment for subjects with advanced cancers per *https://clinicaltrials.gov* (NCT05226507; last accessed October 24, 2022).

We theorize that in our mouse HB model, YAP1 expression leads to the dedifferentiation of hepatocytes to more hepatoblastoma-like cells. β-Catenin then acts as a cellular accelerant, leading to increased growth of the transformed cells. This is based on work that showed transfecting mice with different β-catenin mutations dramatically changed the growth velocities of the resulting tumors.[15] We speculate this reprogramming of cells would lead to misfolded proteins and other signs of cellular stress, which would induce HSF1 signaling. When a cell is under stress, it can either repair itself or induce self-destruction via mechanisms including apoptosis. The *in vitro* work showed transfecting HepG2 cells with the dnHSF1 under standard conditions did not significantly inhibit HSP70 transcription (a marker of HSF1 activation). However, when the cells were heat shocked, transfection with dnHSF1 halved the increase in HSP70 transcription. These studies indicate that the cytotoxic stress increases when tumor cells transition to less differentiated forms. This is suggested by the human

transcriptomic data analysis, showing embryonic tumors have higher HSF1 signaling levels than fetal-appearing tumors.

We speculate this increased cytotoxic stress would lead to induction of apoptosis in cells. Interestingly, HSF1 itself and its individual target genes have been shown to inhibit apoptosis. HSP27 has been shown to inhibit apoptosis via interacting with death domain−associated protein, bcl-2−like protein 4, cytochrome *c*, and caspases under stressful conditions.[55−58] HSP70 blocks assembly of the apoptotic machinery.[59] HSP90 regulates expression of hypoxia-inducible factor-1α in hepatocellular carcinoma.[60] HSF1 itself has been shown to down-regulate second mitochondria-derived activator of caspase (SMAC) to inhibit apoptosis in pancreatic cancer cells.[61] Silencing of HSF1 induced apoptosis in human hepatocellular carcinoma cell lines.[23] dnHSF1-β-Y mice showed a nearly threefold increase in apoptosis 2 weeks after injection compared with β-Y mice. We posit treatment with the dnHSF1 acts as a molecular prune to the burgeoning tumor cells. In most cases, tumor foci do not form. In a few cases, tumor foci persist but are throttled in their growth by HSF1 inhibition. More research is needed to precisely ascertain which downstream targets of HSF1 control apoptosis in hepatoblastoma. In addition, HSF1 signaling may have molecular roles beyond control of apoptosis in hepatoblastoma as it has in other cancers.

This work provides evidence that HSF1 may be a novel biomarker and pharmacologic target for hepatoblastoma. A key question to be explored is whether HSF1 signaling can be inhibited sufficiently to decrease tumor growth while still allowing normal cellular function to minimize adverse effects.

Supplemental Data

Supplemental material for this article can be found at *http://doi.org/10.1016/j.ajpath.2022.10.006*.

References

1. Pham TA, Gallo AM, Concepcion W, Esquivel CO, Bonham CA: Effect of liver transplant on long-term disease-free survival in children with hepatoblastoma and hepatocellular cancer. JAMA Surg 2015, 150:1150−1158
2. Feng J, Polychronidis G, Heger U, Frongia G, Mehrabi A, Hoffmann K: Incidence trends and survival prediction of hepatoblastoma in children: a population-based study. Cancer Commun 2019, 39:62
3. Trobaugh-Lotrario AD, Meyers RL, Tiao GM, Feusner JH: Pediatric liver transplantation for hepatoblastoma. Transl Gastroenterol Hepatol 2016, 1:44
4. Allan BJ, Parikh PP, Diaz S, Perez EA, Neville HL, Sola JE: Predictors of survival and incidence of hepatoblastoma in the paediatric population. HPB (Oxford) 2013, 15:741−746
5. Mussa A, Duffy KA, Carli D, Ferrero GB, Kalish JM: Defining an optimal time window to screen for hepatoblastoma in children with Beckwith-Wiedemann syndrome. Pediatr Blood Cancer 2019, 66: e27492
6. Trobaugh-Lotrario AD, López-Terrada D, Li P, Feusner JH: Hepatoblastoma in patients with molecularly proven familial adenomatous polyposis: clinical characteristics and rationale for surveillance screening. Pediatr Blood Cancer 2018, 65:e27103
7. Bläker H, Hofmann WJ, Rieker RJ, Penzel R, Graf M, Otto HF: Beta-Catenin accumulation and mutation of the CTNNB1 gene in hepatoblastoma. Genes Chromosomes Cancer 1999, 25:399−402
8. de La Coste A, Romagnolo B, Billuart P, Renard C-A, Buendia M-A, Soubrane O, Fabre M, Chelly J, Beldjord C, Kahn A, Perret C: Somatic mutations of the [beta]-catenin gene are frequent in mouse and human hepatocellular carcinomas. Proc Natl Acad Sci U S A 1998, 95:8847
9. Bell D, Ranganathan S, Tao J, Monga SPS: Novel advances in understanding of molecular pathogenesis of hepatoblastoma: a Wnt/[beta]-catenin perspective. Gene Expr 2017, 17:141
10. Cairo S, Armengol C, De Reyniès A, Wei Y, Thomas E, Renard CA, et al: Hepatic stem-like phenotype and interplay of Wnt/[beta]-catenin and Myc signaling in aggressive childhood liver cancer. Cancer Cell 2008, 14:471−484
11. Tao J, Calvisi DF, Ranganathan S, Cigliano A, Zhou L, Singh S, Jiang L, Fan B, Terracciano L, Armeanu-Ebinger S, Ribback S, Dombrowski F, Evert M, Chen X, Monga SPS: Activation of [beta]-catenin and Yap1 in human hepatoblastoma and induction of hepatocarcinogenesis in mice. Gastroenterology 2014, 147:690−701
12. Camargo FD, Gokhale S, Johnnidis JB, Fu D, Bell GW, Jaenisch R, Brummelkamp TR: YAP1 increases organ size and expands undifferentiated progenitor cells. Curr Biol 2007, 17:2054−2060
13. Piccolo S, Dupont S, Cordenonsi M: The biology of YAP/TAZ: hippo signaling and beyond. Physiol Rev 2014, 94:1287−1312
14. Min Q, Molina L, Li J, Adebayo Michael AO, Russell JO, Preziosi ME, Singh S, Poddar M, Matz-Soja M, Ranganathan S, Bell AW, Gebhardt R, Gaunitz F, Yu J, Tao J, Monga SP: [beta]-Catenin and Yes-associated protein 1 cooperate in hepatoblastoma pathogenesis. Am J Pathol 2019, 189:1091−1104
15. Zhang W, Meyfeldt J, Wang H, Kulkarni S, Lu J, Mandel JA, Marburger B, Liu Y, Gorka JE, Ranganathan S, Prochownik EV: [beta]-Catenin mutations as determinants of hepatoblastoma phenotypes in mice. J Biol Chem 2019, 294:17524−17542
16. Dai C, Whitesell L, Rogers AB, Lindquist S: Heat shock factor 1 is a powerful multifaceted modifier of carcinogenesis. Cell 2007, 130: 1005−1018
17. Mendillo ML, Santagata S, Koeva M, Bell GW, Hu R, Tamimi RM, Fraenkel E, Ince TA, Whitesell L, Lindquist S: HSF1 drives a transcriptional program distinct from heat shock to support highly malignant human cancers. Cell 2012, 150:549−562
18. Calderwood SK: Elevated levels of HSF1 indicate a poor prognosis in breast cancer. Future Oncol 2012, 8:399−401
19. Cen H, Zheng S, Fang YM, Tang XP, Dong Q: Induction of HSF1 expression is associated with sporadic colorectal cancer. World J Gastroenterol 2004, 10:3122−3126
20. Cui J, Tian H, Chen G: Upregulation of nuclear heat shock factor 1 contributes to tumor angiogenesis and poor survival in patients with non-small cell lung cancer. Ann Thorac Surg 2015, 100:465−472
21. Ritossa F: A new puffing pattern induced by temperature shock and DNP in drosophila. Experientia 1962, 18:571−573
22. Fang F, Chang R, Yang L: Heat shock factor 1 promotes invasion and metastasis of hepatocellular carcinoma in vitro and in vivo. Cancer 2012, 118:1782−1794
23. Cigliano A, Wang C, Pilo MG, Szydlowska M, Brozzetti S, Latte G, Pes GM, Pascale RM, Seddaiu MA, Vidili G, Ribback S, Dombrowski F, Evert M, Chen X, Calvisi DF: Inhibition of HSF1 suppresses the growth of hepatocarcinoma cell lines in vitro and AKT-driven hepatocarcinogenesis in mice. Oncotarget 2017, 8: 54149−54159

24. Cigliano A, Pilo MG, Li L, Latte G, Szydlowska M, Simile MM, Paliogiannis P, Che L, Pes GM, Palmieri G, Sini MC, Cossu A, Porcu A, Vidili G, Seddaiu MA, Pascale RM, Ribback S, Dombrowski F, Chen X, Calvisi DF: Deregulated c-Myc requires a functional HSF1 for experimental and human hepatocarcinogenesis. Oncotarget 2017, 8:90638
25. Zhang S, Zhang J, Evert K, Li X, Liu P, Kiss A, Schaff Z, Ament C, Zhang Y, Serra M, Evert M, Chen N, Xu F, Chen X, Tao J, Calvisi DF, Cigliano A: The hippo effector transcriptional coactivator with PDZ-binding motif cooperates with oncogenic [beta]-catenin to induce hepatoblastoma development in mice and humans. Am J Pathol 2020, 190:1397−1413
26. Li Q, Martinez JD: Loss of HSF1 results in defective radiation-induced G2 arrest and DNA repair. Radiat Res 2011, 176:17
27. Lu M, Park J-S: Protonation behavior of histidine during HSF1 activation by physiological acidification. J Cell Biochem 2015, 116: 977−984
28. Molina L, Yang H, Adebayo Michael AO, Oertel M, Bell A, Singh S, Chen X, Tao J, Monga SPS: MTOR inhibition affects Yap1-[beta]-catenin-induced hepatoblastoma growth and development. Oncotarget 2019, 10:1475−1490
29. Wang Y, Theriault JR, He H, Gong J, Calderwood SK: Expression of a dominant negative heat shock factor-1 construct inhibits aneuploidy in prostate carcinoma cells. J Biol Chem 2004, 279:32651−32659
30. Molina L, Bell D, Tao J, Preziosi M, Pradhan-Sundd T, Singh S, Poddar M, Luo J, Ranganathan S, Chikina M, Monga SP: Hepatocyte-derived lipocalin 2 is a potential serum biomarker reflecting tumor burden in hepatoblastoma. Am J Pathol 2018, 188:1895−1909
31. Barrett T, Wilhite SE, Ledoux P, Evangelista C, Kim IF, Tomashevsky M, Marshall KA, Phillippy KH, Sherman PM, Holko M, Yefanov A, Lee H, Zhang N, Robertson CL, Serova N, Davis S, Soboleva A: NCBI GEO: archive for functional genomics data sets - update. Nucleic Acids Res 2013, 41:D991−D995
32. Athar A, Füllgrabe A, George N, Iqbal H, Huerta L, Ali A, Snow C, Fonseca NA, Petryszak R, Papatheodorou I, Sarkans U, Brazma A: ArrayExpress update - from bulk to single-cell expression data. Nucleic Acids Res 2019, 47:D711−D715
33. Hiyama E, Ueda Y, Kurihara S, Kawashima K, Ikeda K, Morihara N, Fukazawa T, Kanawa M, Hiyama K: Gene expression profiling in hepatoblastoma cases of the Japanese Study Group for Pediatric Liver Tumors-2 (JPLT-2) trial. Eur J Mol Cancer 2019, 1:1−8
34. Sumazin P, Chen Y, Treviño LR, Sarabia SF, Hampton OA, Patel K, Mistretta TA, Zorman B, Thompson P, Heczey A, Comerford S, Wheeler DA, Chintagumpala M, Meyers R, Rakheja D, Finegold MJ, Tomlinson G, Parsons DW, López-Terrada D: Genomic analysis of hepatoblastoma identifies distinct molecular and prognostic subgroups. Hepatology 2017, 65:104−121
35. Valanejad L, Cast A, Wright M, Bissig KD, Karns R, Weirauch MT, Timchenko N: PARP1 activation increases expression of modified tumor suppressors and pathways underlying development of aggressive hepatoblastoma. Commun Biol 2018, 1:67
36. Hooks KB, Audoux J, Fazli H, Lesjean S, Ernault T, Dugot-Senant N, Leste-Lasserre T, Hagedorn M, Rousseau B, Danet C, Branchereau S, Brugières L, Taque S, Guettier C, Fabre M, Rullier A, Buendia MA, Commes T, Grosset CF, Raymond AA: New insights into diagnosis and therapeutic options for proliferative hepatoblastoma. Hepatology 2018, 68:89−102
37. Ranganathan S, Ningappa M, Ashokkumar C, Higgs BW, Min J, Sun Q, Schmitt L, Subramaniam S, Hakonarson H, Sindhi R: Loss of EGFR-ASAP1 signaling in metastatic and unresectable hepatoblastoma. Sci Rep 2016, 6:38347
38. Fisher R: Statistical Methods for Research Workers. Edinburgh, Scotland, Genesis Publishing, Oliver and Boyd; Biol. Monogr. Manuals, 1925
39. Livak KJ, Schmittgen TD: Analysis of relative gene expression data using real-time quantitative PCR and the 2-ΔΔCT method. Methods 2001, 25:402−408
40. Cairo S, Armengol C, Buendia MA: Activation of Wnt and Myc signaling in hepatoblastoma. Front Biosci 2012, 4:480−486
41. Chang LC, Lin HM, Sibille E, Tseng GC: Meta-analysis methods for combining multiple expression profiles: comparisons, statistical characterization and an application guideline. BMC Bioinformatics 2013, 14:368
42. Kiruthiga KG, Ramakrishna B, Saha S, Sen S: Histological and immunohistochemical study of hepatoblastoma: correlation with tumour behaviour and survival. J Gastrointest Oncol 2018, 9:326
43. Qiao G, Chen Z, Wang C, Ge J, Zhang Z, Li L, Ren J: Pure fetal histology subtype was associated with better prognosis of children with hepatoblastoma: a Chinese population-based study. J Gastroenterol Hepatol 2016, 31:621−627
44. Wang H, Lu J, Edmunds LR, Kulkarni S, Dolezal J, Tao J, Ranganathan S, Jackson L, Fromherz M, Beer-Stolz D, Uppala R, Bharathi S, Monga SP, Goetzman ES, Prochownik EV: Coordinated activities of multiple Myc-dependent and Myc-independent biosynthetic pathways in hepatoblastoma. J Biol Chem 2016, 291: 26241−26251
45. Ranganathan S, Tan X, Monga SPS: [beta]-Catenin and met deregulation in childhood hepatoblastomas. Pediatr Dev Pathol 2005, 8: 435−447
46. Donna BS, Wang H, Lu J, Edmunds LR, Kulkarni S, Dolezal J, Tao J, Ranganathan S, Jackson L, Fromherz M, Uppala R, Bharathi S, Monga SP, Goetzman ES, Prochownik EV: Coordinated activities of multiple myc-dependent and myc-independent biosynthetic pathways in hepatoblastoma. J Biol Chem 2016, 291:26241−26251
47. Reggiani F, Gobbi G, Ciarrocchi A, Sancisi V: YAP and TAZ are not identical twins. Trends Biochem Sci 2021, 46:154−168
48. Johnson ML, Yu HA, Hart EM, Weitner BB, Rademaker AW, Patel JD, Kris MG, Riely GJ: Phase I/II study of HSP90 inhibitor AUY922 and erlotinib for EGFR-mutant lung cancer with acquired resistance to epidermal growth factor receptor tyrosine kinase inhibitors. J Clin Oncol 2015, 33:1666−1673
49. Dhingra K, Valero V, Gutierrez L, Theriault R, Booser D, Holmes F, Buzdar A, Fraschini G, Hortobagyi G: Phase II study of deoxyspergualin in metastatic breast cancer. Invest New Drugs 1994, 12: 235−241
50. Propper DJ, Braybrooke JP, Taylor DJ, Lodi R, Styles P, Cramer JA, Collins WCJ, Levitt NC, Talbot DC, Ganesan TS, Harris AL: Phase I trial of the selective mitochondrial toxin MKT 077 in chemo-resistant solid tumours. Ann Oncol 1999, 10:923−927
51. Lelj-Garolla B, Kumano M, Beraldi E, Nappi L, Rocchi P, Ionescu DN, Fazli L, Zoubeidi A, Gleave ME: Hsp27 inhibition with OGX-427 sensitizes non−small cell lung cancer cells to erlotinib and chemotherapy. Mol Cancer Ther 2015, 14:1107−1116
52. Rosenberg JE, Hahn NM, Regan MM, Jacobs C, Stewart PS, Choueiri TK: The Borealis-2 clinical trial: a randomized phase II study of OGX-427 plus docetaxel versus docetaxel alone in relapsed/refractory metastatic urothelial cancer. Am Soc Clin Oncol 2013, 31:TPS4588
53. Yoon YJ, Kim JA, Shin KD, Shin DS, Han YM, Lee YJ, Lee JS, Kwon BM, Han DC: KRIBB11 inhibits HSP70 synthesis through inhibition of heat shock factor 1 function by impairing the recruitment of positive transcription elongation factor b to the hsp70 promoter. J Biol Chem 2011, 286:1737−1747
54. Dong B, Jaeger AM, Hughes PF, Loiselle DR, Spencer Hauck J, Fu Y, Haystead TA, Huang J, Thiele DJ: Targeting therapy-resistant prostate cancer via a direct inhibitor of the human heat shock transcription factor 1. Sci Transl Med 2020, 12:eabb5647
55. Charette SJ, Landry J: The interaction of HSP27 with Daxx identifies a potential regulatory role of HSP27 in Fas-induced apoptosis. Ann N Y Acad Sci 2000, 926:126−131
56. Calderwood SK, Khaleque MA, Sawyer DB, Ciocca DR: Heat shock proteins in cancer: chaperones of tumorigenesis. Trends Biochem Sci 2006, 31:164−172

57. Havasi A, Li Z, Wang Z, Martin JL, Botla V, Ruchalski K, Schwartz JH, Borkan SC: Hsp27 inhibits Bax activation and apoptosis via a phosphatidylinositol 3-kinase-dependent mechanism. J Biol Chem 2008, 283:12305−12313
58. Bruey JM, Ducasse C, Bonniaud P, Ravagnan L, Susin SA, Diaz-Latoud C, Gurbuxani S, Arrigo AP, Kroemer G, Solary E, Garrido C: Hsp27 negatively regulates cell death by interacting with cytochrome c. Nat Cell Biol 2000, 2:645−652
59. Beere HM, Wolf BB, Cain K, Mosser DD, Mahboubi A, Kuwana T, Tailor P, Morimoto RI, Cohen GM, Green DR: Heat-shock protein 70 inhibits apoptosis by preventing recruitment of procaspase-9 to the Apaf-1 apoptosome. Nat Cell Biol 2000, 2:469−475
60. Liu X, Chen S, Tu J, Cai W, Xu Q: HSP90 inhibits apoptosis and promotes growth by regulating HIF-1[alpha] abundance in hepatocellular carcinoma. Int J Mol Med 2016, 37:825−835
61. Liang W, Liao Y, Zhang J, Huang Q, Luo W, Yu J, Gong J, Zhou Y, Li X, Tang B, He S, Yang J: Heat shock factor 1 inhibits the mitochondrial apoptosis pathway by regulating second mitochondria-derived activator of caspase to promote pancreatic tumorigenesis. J Exp Clin Cancer Res 2017, 36:1−14